PHYSICAL REVIEW B

CONDENSED MATTER

THIRD SERIES, VOLUME 38, NUMBER 16 PART A 1 DECEMBER 1988

Electronic sputtering of condensed O_2

K. M. Gibbs
Department of Nuclear Engineering and Engineering Physics, University of Virginia, Charlottesville, Virginia 22901

W. L. Brown
AT&T Bell Laboratories, Murray Hill, New Jersey 07974

R. E. Johnson
Department of Nuclear Engineering and Engineering Physics, University of Virginia, Charlottesville, Virginia 22901

(Received 21 June 1988)

The electronically induced sputtering of solid oxygen films has been measured using helium and hydrogen ions with energies from 0.3 to 3.5 MeV. The sputtering yield exhibits a linear dependence on $(dE/dx)_e$, the electronic stopping power of the ions, at low $(dE/dx)_e$, with a transition to an approximately quadratic dependence at high $(dE/dx)_e$. These results are similar to those found for solid N_2 but differ from those for solid CO. The electronic sputtering yield of oxygen has also been measured as a function of the angle of incidence of singly charged and charge-state-equilibrated helium ions at 2 MeV. The angular dependence of the yield is approximately $(\cos\theta)^{-1.6}$ and is essentially the same for both the singly charged and equilibrated ions, although the absolute yields are a factor of 1.2 higher for the charge-state-equilibrated ions. The measured angular dependence in the quadratic sputtering regime is remarkably well accounted for by a model of diffusive energy transport to the surface and sputtering by a collective process.

I. INTRODUCTION

Sputtering may be produced as a result of energy deposited in a material in either of two ways. The first, due to direct energy transfer from elastic nuclear collisions between the incident ion and the target atom nuclei, is called collisional sputtering. The second results from the conversion of energy deposited as electronic ionization and excitation of the target atoms into nuclear motion. This is called electronic sputtering. It does not occur in metals but has been observed in a number of insulating solids, particularly in condensed gases. Collisional sputtering has been extensively studied, and is well understood both qualitatively and quantitatively for metallic atomic targets.[1] Interest in the electronic sputtering regime over the last ten years was stimulated by experiments in which energetic (MeV regime) ions incident on H_2O ice gave a sputtering yield, Y_s, versus ion energy that clearly followed the electronic stopping power.[2] While several models have been proposed to explain the electronic sputtering effect,[3-5] there is still no comprehensive theory that predicts the yield.

Work on the electronically induced sputtering of low-temperature molecular-gas solids such as CO_2 (Ref. 6), CO (Ref. 7), SO_2 (Ref. 8), H_2O (Ref. 9). N_2 (Refs. 10 and 12), O_2 (Refs. 11 and 12), and CH_4 (Ref. 13) has been reported. Because oxygen is a simple diatomic molecular system, oxygen ice at 10 K was chosen for the present study of the electronic sputtering process to elucidate further the mechanisms that cause sputtering. The sputtering yield has been measured as a function of the electronic stopping power of MeV-energy H and He ions. These results are compared with those for N_2 and CO at 10 K. The sputtering yield of O_2 has also been measured as a function of the angle of incidence of an ion beam in order to test the idea that the angular dependence is affected by the near-surface depth dependence of the energy-deposition rate.[14]

II. EXPERIMENTAL METHOD

The condensed oxygen targets were prepared by directing a flow of room-temperature oxygen gas onto a copper substrate which was cryogenically cooled to ~ 10 K. The gas flow passed through a microchannel plate which divided the flow into hundreds of thousands of very small streams to ensure uniform deposition over a circle approximately 1.25 cm in diameter. In the present experiments the films used were about 2 μm in thickness. The targets were grown in an ultrahigh vacuum chamber and

the copper substrate (attached to a liquid-helium transport cryostat) could be rotated to vary the angle of incidence of the ion beam. Figure 1 is a schematic diagram of the experimental apparatus. The source of the MeV ions used for this study was a 3.75-MeV Van de Graaff accelerator.

For measurements of the stopping-power dependence of the sputtering yield, a quadrupole mass spectrometer (QMS) was used with ions always perpendicularly incident on the target. Measurements were made with 0.3–3.5 MeV H^+ and 1.0–3.0-MeV He^+ at various energies. The beams were collimated with a 3-mm diameter aperture. For He^+ ions a beam current of 50 nA was sufficient to induce an easily measurable sputtering yield. However, for H^+ ions, beam currents $\sim$200 nA were required. In both cases it was determined that the sputtering yield was independent of the beam current to currents well beyond these values (i.e., there was no macroscopic heating effect). Measurements were also made with equilibrium charge state helium ions He^{q+}. The equilibrium charge state was achieved by using a 20-$\mu g/cm^2$ carbon foil mounted on the 3-mm diameter collimating aperture. Scattering of the ion beam by the foil was determined to be insignificant for these experiments.

Because of the strong angular bias in the quadrupole response to sputtering at different target orientations, the total pressure increase in the ice chamber was used to measure the angular dependence of Y_s. The ionization gauge was mounted on the side of the ice chamber directly opposite the incident ion beam so that all ejected molecules required many collisions to reach it and the results should be symmetric for positive and negative angles. The cryopump for the chamber was located below the target and thus provided equivalent pumping no matter what the direction of molecular ejection from the target. An analog signal from the ionization gauge control unit was used as a relative measure of the sputtering yield, and the results obtained were free from the angular bias observed with the QMS.

The ion beam incident on the target surface was pulsed on and off using a set of electrostatic deflection plates. During the "off" periods the target was rotated to the next angle of incidence and the background pressure was simultaneously measured. Figure 2 shows a representative run. The difference between the "on" and "off" pressure measurements is proportional to the relative sputtering yield at the various angles of incidence. The relative yield is defined as the pressure change divided by the beam current in each measurement. The angular dependence was measured for 2-MeV He^+ and equilibrium charge state helium ions, He^{q+}.

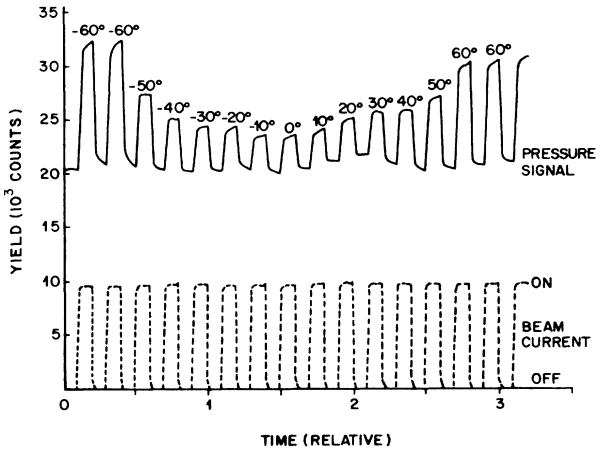

FIG. 2. Representative data for the angular dependence of the sputtering yield using the output of the ionization gauge to indicate the total sputtering yield at each angle. The ion beam is pulsed on and off as shown in the lower trace in the figure, the angle of the target to the beam being changed during off periods of the cycle.

Both the ion gauge and QMS measure only relative sputtering yields. The absolute yield (molecules per ion)[12] has been determined from Rutherford backscattering (RBS) measurements described in Refs. 2 and 9. Thus, the normal incidence value of the yield for the ion gauge and for the QMS can be normalized to the RBS value.

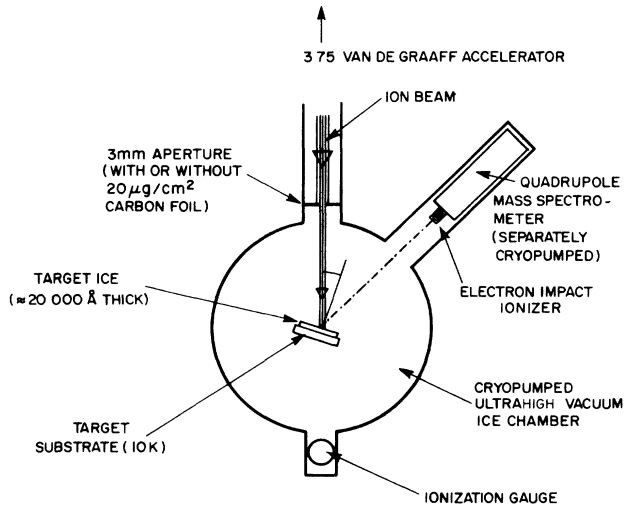

FIG. 1. Schematic diagram of apparatus.

III. STOPPING-POWER DEPENDENCE

A. Experimental results

The results of the stopping-power dependence of the sputtering yields are shown in Fig. 3 for incident H^+ and He^+. The yield for He^{q+} at 2 MeV is also shown. The relative sputtering yields, measured with the QMS, were normalized to the RBS yield of 54±5 molecules ejected per incident ion for 2-MeV He^+ (Ref. 12). The sputtering yield in the region of $(dE/dx)_e$ close to that of 2-MeV He^+ exhibits the same, roughly quadratic, dependence on the $(dE/dx)_e$ observed for several other low-temperature condensed molecular gases H_2O, (Ref. 9), N_2 (Ref. 10), and CO (Ref. 7). However, the yield also exhibits a transition to an approximately linear dependence on the stopping power at low $(dE/dx)_e$. This is very similar to the variation found in solid N_2 (Ref. 10), but the transition region is shifted to lower $(dE/dx)_e$ by a factor of 2–3 compared with N_2.

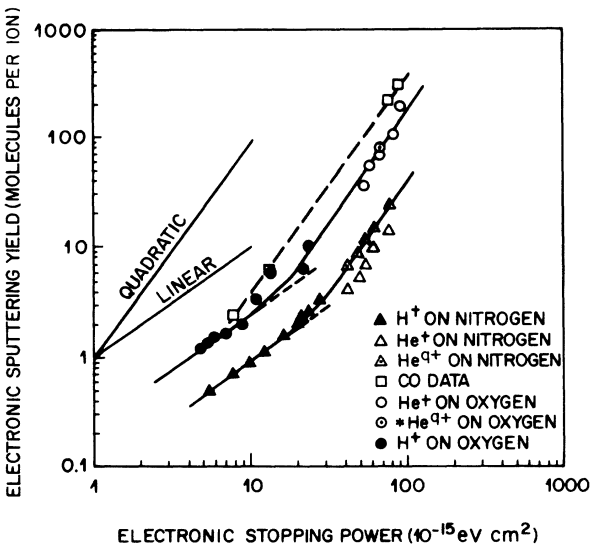

FIG. 3. Yields in molecules ejected per ion incident vs the electronic stopping power for protons and helium ions on solid CO, O_2, and N_2 at ~ 10 K. Circles are the new data for condensed O_2. Lines are drawn to guide the eye. Linear and quadratic dependences are indicated by the lines at the left of the figure.

B. Discussion

The linear dependence of sputtering yield at low $(dE/dx)_e$ is consistent with the keV-electron sputtering results of Ellegaard *et al.*[11] which are also at low $(dE/dx)_e$ although quantitative agreement in absolute yield for the same effective $(dE/dx)_e$ has not been found. The existence of a linear regime allows a description of the sputtering in terms of independent excitations produced along the track of a single particle. The quadratic regime still involves single particles (the yield is independent of ion beam current density) and the quadratic dependence must arise from cooperative effects of independent excitation events along the path of an individual particle.[3,5]

The absolute yields in the linear regime in Fig. 3 are about 2.6 times the yields at the same $(dE/dx)_e$ for N_2. This is slightly larger than the factor of 2.3 which can be deduced from the results of Rook *et al.*[12] for O_2 and N_2 sputtering in the quadratic regime. The ratio is also in approximate agreement with the electron sputtering data of Ellegaard *et al.*[11] Sputtering yields in the linear regime are expected to be roughly proportional to the electronic energy impulsively converted to kinetic energy of motion per ionization along the path of an individual ion, and inversely proportional to the surface binding energy.[3–5,10] Since the cohesive energy of O_2 is larger than that of N_2 by a factor of 1.26, we conclude that the impulsive energy conversion is approximately three times as large in solid O_2 as in N_2.

The position of the transition region from linear to quadratic in $(dE/dx)_e$ for O_2 occurs a factor of 2–3 below that for N_2. This is consistent with the idea that the transition is due to the same process in the two systems with a higher energy conversion per ionization driving the transitions in the O_2 case.

In Fig. 3 it is also seen that the He^{q+} yields are slightly higher than the He^+ yields. The sign of this difference is expected because an incident MeV He^{q+} ion with $q>1$ is expected to deposit a greater amount of energy near the surface than an He^+ ion does. As the He^+ penetrates into the solid its charge-state changes toward the equilibrium value, after which the energy deposition will be the same as for the incident charge equilibrated ion. The average charge state q was measured to be 1.75 in the present experiments for 2-MeV He. It is interesting that the yield ratio is only 1.2. This is much smaller than the $(1.75)^4$ that might be expected in this region, where the sputtering process is quadratic in energy deposition (which scales as q^2) and if only the energy deposition by the incident ion at the surface were contributing to sputtering. The smallness of the experimental ratio suggests either (1) that the differences in energy deposition are not as large as expected by simply comparing incident ion charge, (2) that charge-state equilibration occurs very close to the surface, or (3) that considerable redistribution of the electronically deposited energy takes place prior to the electronic-to-kinetic energy conversion that leads to sputtering.

In estimating energy deposition differences we note that the measured gas-phase stopping cross-section ratio for He^{2+} and He^+ on H_2O is ~ 1.2 (Ref. 15), much smaller then the factor of 4 which is the ratio of the charges squared. Furthermore, the stopping cross section (i.e., first-layer stopping power) for H is calculated to be *larger* than that for H^- (Ref. 16) at high velocities. In these cases, the electron that is associated with the H atom or the He^+ ion also provides ionization when the ion or atom velocity is large compared with the velocity of the bound electron. If N is the number of electrons and Z is the nuclear charge, the result can be expressed[16] as

$$Z_{\text{eff}}^2=[Z^2+(Z-N)^2+N]/2\ . \tag{1}$$

From this expression, $Z_{\text{eff}}\sim 1.73$ for He^+ and $Z_{\text{eff}}\sim 1.94$ for He^{q+} (where the He^{q+} value is deduced as the appropriately weighted sum of Z_{eff} for He^{2+} and He^+). These Z_{eff}'s allow comparison of the energy deposition in the first layer of the target before any charge-state equilibrium has taken place. Ignoring the other corrections to the stopping cross-section calculation,[16] these Z_{eff}'s would predict a yield ratio of ~ 1.5. This is much closer to the measured yield ratio than $(1.75)^4$. A further reduction in this calculated ratio will result if charge-state equilibration occurs very close to the surface in a depth comparable to that from which sputtering can occur. This latter depth is estimated to be only ~ 4 monolayers.[17] The charge-state equilibration depth expected on the basis of gas-phase results is ~ 15 monolayers.[14,18] It may be shorter due to multiple excitations in the rapid successive collisions in a solid target. The effective charge-state yield ratio may also be reduced if there is redistribution of electronically deposited energy prior to its conversion to kinetic energy of the atoms. This trans-

port length is not known, but the distances which are significant in the problem are so short ($\sim$4–15 monolayers) that redistribution may well be important.

The measured yield ratio above allows an estimate to be made of the energy distribution in depth at the time of sputtering. In the quadratic sputtering regime

$$[Y_s(0)^{q+}/Y_s(0)^{1+}]-1\approx 2[\Delta(1+)-\Delta(q+)]\approx 0.2\ , \quad (2)$$

where $\Delta(q+)$ and $\Delta(1+)$ are the fractional deficits in the final kinetic energy conversion at the surface compared with that deep in the material for the $q+$ or $1+$ case, respectively.[14] Because the $q+$ ion is already in its "equilibrium" charge state, $\Delta(q+)$ is expected to be smaller than $\Delta(1+)$ so that we estimate $\Delta(1+)\approx 0.1$, a quantity we will use later.

IV. ANGULAR-DEPENDENCE MEASUREMENTS

A. Experimental results

When the angle of incidence is varied from perpendicular, more energy is deposited per unit depth by each incident ion. In agreement with expectations, this produces an increase in the sputtering yield. Figures 4(a) and 4(b) represent the angular dependences for the nonequilibrated and equilibrated helium ion beams, respectively. The yield in Fig. 4(a) is (Δp/beam current) in relative units. In Fig. 4(b) it is $(\Delta p/I_B/q)$ where I_B is the beam current. Thus, both 4(a) and 4(b) present the sputtering effectiveness per particle (rather than per unit incident charge). $Y_s(0)$ in Eq. (2) for He^{q+} is a factor of 1.2 larger than that for He^+, as noted in Sec. III B. The solid curves in Fig. 4 are least square fits of the data to the function

$$Y_s(\theta)=Y_s(0)/\cos^n(\theta+\beta)\ . \quad (3)$$

In this expression n, β, and $Y_s(0)$ are fitting parameters where $Y_s(0)$ is the yield at perpendicular incidence, β is the zero offset angle, and n is the exponent of the cosine. Typical values of β were found to be less than 1°. The fit of this functional form to the data is seen to be quite satisfactory with values of $n=1.63\pm 0.09$ for both He^+ and He^{q+} incident ions.

B. Discussion

The magnitude of the exponent of $\cos\theta$ and its similarity for He^+ and He^{q+} were initially a surprise. A similar value for n ($\sim$1.6) had been reported for 1.5-MeV He^+ incident on CO at 10 K (Ref. 7). This was qualitatively interpreted as being associated with the nonlinearity in the sputter yield. However, Johnson *et al.*[14] showed that a depth dependence in the energy deposition could lead to an angular dependence different from $\cos(\theta)^{-1}$, and, in fact, differing angular dependences with differing charge states have been observed for heavier ions on organic solids.[19] From the estimate in Ref. 14, $n\leq 1+(2\Delta)\bar{z}_s/\bar{z}$ where Δ is the fractional deficit in the energy deposition at the surface [as in Eq. (2)], $\bar{z}$ is the charge-state equilibration depth (or the diffusion length of excited states, whichever is larger), and $\bar{z}_s$ is the depth contributing to sputtering. Sputtering originating from electronic-to-kinetic energy-conversion events is typically produced at depths of the order of 4 monolayers or less;[18] thus $\bar{z}_s/\bar{z}$ is less than unity. Since $\Delta(q+)$ is small and $\Delta(1+)$ is at most only 0.1, as determined earlier, it is impossible to account for an $n=1.6$ in this way. The difference in the n values for the $q+$ and $1+$ cases is smaller than the estimate in Ref. 4 but both values of n differ significantly from 1.

In the quadratic sputtering regime "spike" models have been shown to be useful for parametrizing the yield.[20–23] For calculating the angular-dependent conse-

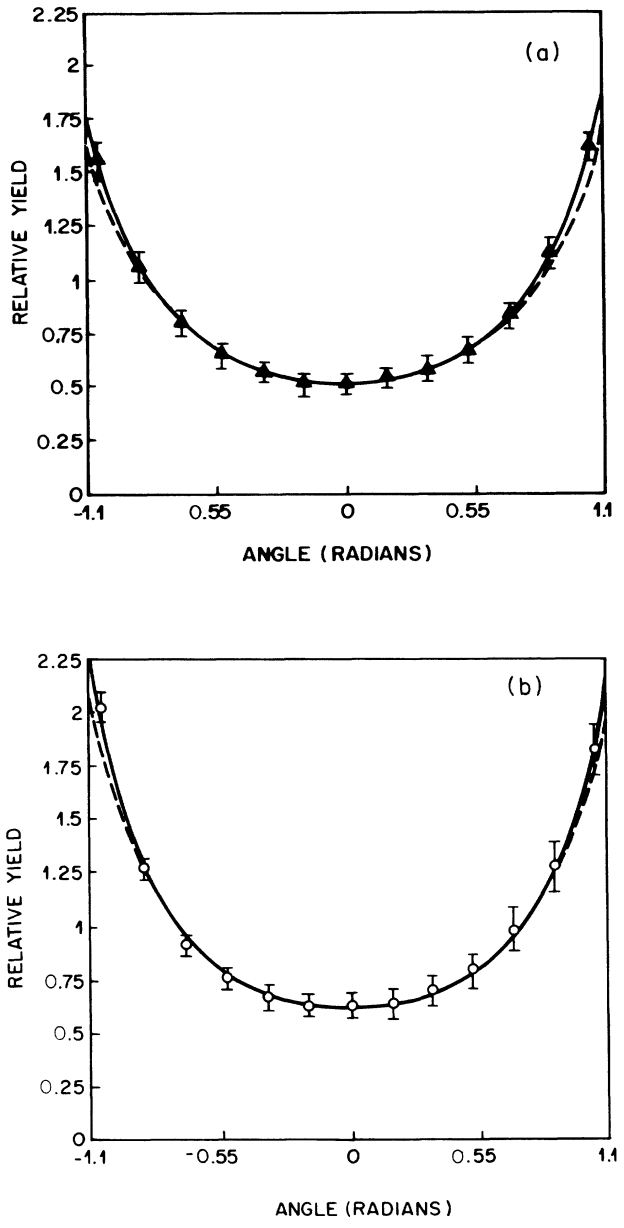

FIG. 4. (a) Relative sputtering yield (see the text) vs incident angle θ for 2-MeV He^+. Solid line is a fit to Eq. (3) with $n=1.64$ and $\beta=0.6°$. Dashed line from Eq. (4). (b) Same as in (a) for He^{q+}, $n=1.63$, and $\beta=-0.2°$.

quences of such a model we imagine each excitation along an ion track contributes by diffusive energy transport to the ejection process at the surface which we assume depends on the local surface energy density. For a thermal-spike model[22] and a shock model,[24] estimates of $n \approx 1.5$ have been obtained. In the Appendix we derive an analytic expression for the case in which the diffusivity is constant and the energy deposition is uniform along the track. The result is

$$Y(\theta)=Y(0)\left[\frac{4}{\pi}\frac{1}{\cos\theta}\tan^{-1}\left[\frac{1}{\cos\theta}\right]\right] . \quad (4)$$

Near $\cos\theta \approx 1$, this gives a $\cos\theta^{-n}$ dependence with $n=1+2/\pi=1.64$, remarkably close to the results shown in Figs. 4(a) and 4(b). In fact, over the whole angular range studied, the measured yields are nearly fit by the angular dependence in Eq. (3) as seen from the dashed curves in Fig. 4. It is interesting that this form results if the yield is simply assumed to be quadratic in the additive contributions (at the surface) from individual events along the particle path (see the Appendix).

V. SUMMARY

It has been shown that the electronic sputtering yield for O_2 by MeV energy ions exhibits a transition from a linear to quadratic dependence on the electronic stopping power. Similar results have been found for the case of N_2 (Ref. 10). Based on the size of the absolute yields and the similarities in the binding energies and ionization rates, the linear yields for O_2 and N_2 indicate that nearly three times the amount of impulsive energy is released in the O_2 case per ionization event. This is similar to the result found for incident keV energy electrons[11] and that deduced from results in the quadratic region for MeV He^+ (Ref. 12). It is interesting that sputtering studies of CO have not yet revealed any transition of the sputtering yield to a linear regime.[7,25]

The observation of a factor of 1.2 between the yields for the equilibrated- and the nonequilibrated-charge-state He beams clearly implies that the near-surface energy deposition density is different for the two beams. However, this ratio is much smaller than that expected based on the relative stopping powers estimated from the ratio of the incident charges. Measurements of helium stopping in water[15] and a simple estimate of effective charge which considers the role of the bound electron[16] suggests a stopping-power ratio ~ 1.2. In the quadratic regime this implies a yield ratio $\sim 1.4-1.5$. A difference in the normal incidence sputtering yield between an MeV He^+ and He^{q+} ion beam was also reported in studies with N_2 (Ref. 10). In that case, the factor was ~ 1.4, close to the preceding estimate. The difference between the factors for O_2 and N_2 is not yet understood, but its sign seems to be consistent with simple expectations for larger impulsive energy inputs in the O_2 case.

It has also been shown that the oxygen sputtering yield depends on the angle of ion incidence as $(\cos\theta)^{-n}$ with $n=1.63\pm0.09$ for both equilibrated and nonequilibrated beams. This dependence is the same as that reported for CO where $n=1.6$ for a nonequilibrated He^+ beam. For the CO case, Johnson *et al.*[14] estimated the increase in n above 1 was due to the depth dependence of the energy deposition caused in roughly equal parts by the equilibration of the incident ions and by the forward directedness of the secondary electrons. The present experiment indicates that at least the first correction is not significant in solid O_2, and, therefore, probably not in CO also. Since the forward directedness of secondary electrons may be the same for both He^+ and He^{q+} beams, its possible role cannot be ruled out by their comparison in the current experiments. However, accounting for an n as large as 1.6 does not appear to be reasonable based on the estimates in Ref. 14.

The apparent invariance of n for He^+ and He^{q+} for O_2, and He^+ for CO, suggests there is an inherent angular dependence that overwhelms the details of spatial energy deposition near the surface. Viewing sputtering as an ejection process dependent on the surface energy density which is contributed additively by ionization events all along the ion's path, gives an angular dependence very close to that found experimentally. Such a model is also consistent with the quadratic dependence of the yield on $(dE/dx)_e$ (Refs. 5 and 22) at the $(dE/dx)_e$ for which the angular dependence was measured. We note that linear collision cascade sputtering produced by direct momentum transferring collisions of low-energy ions also gives an $n=1.6$ (Ref. 1) due to forward directedness of the momentum transfer to the target atoms. Therefore, it will be important to measure the angular dependence of sputtering of N_2 or O_2 in the linear regime of *electronic sputtering* to clarify the validity of the surface-energy activated model which seems to account for the results in the *quadratic regime* very well.

ACKNOWLEDGMENTS

In this work the University of Virginia was supported in part by the National Science Foundation Division of Materials under Grant No. DMR-86-00469. We thank Dr. M. Pospiezalsha for checking the Appendix.

APPENDIX

We evaluate the angular dependence of the yield using diffusive energy transport and an activated surface process often referred to as a cylindrical "spike" model.[20–23,26] In this, the flux of molecules from the surface is stimulated by the total local energy density at the surface $\varepsilon_s(\rho,t)$. The latter quantity is a sum of contributions from assumed point sources along the "track" of the incident ion. Therefore,

$$Y=\int\int d^2\rho \int dt\, \Phi(\varepsilon_s/nU) . \quad (A1)$$

Here, Φ is the stimulation function in response to the ratio of ε_s to the cohesive energy density, nU, where U is the sublimation energy and n is the molecular number density. For this calculation, Φ is assumed to have no explicit time dependence as it would have in an exciton decay model.[27] We also assume the energy spreads from the point of deposition on the track governed by the diffusion equation using, for simplicity, constant

diffusivity κ. Therefore, each element of the track $(dz/\cos\theta)$, where θ is the angle of the track to the normal and z is depth, contributes an amount of energy

$$[f_e(dE/dx)_e](dz/\cos\theta)$$

which distributes isotropically according to

$$e^{-r^2/4\kappa t}/(4\pi\kappa t)^{3/2} .$$

Here, f_e is the fraction of $(dE/dx)_e$ which is converted to energy of atomic motion.[3,5,12] Therefore,

$$\varepsilon_s(\rho,t)=\beta f_e\left[\frac{dE}{dx}\right]_e\frac{1}{\cos\theta}\int_0^\infty dz\frac{e^{-r^2/4\kappa t}}{(4\pi\kappa t)^{3/2}} , \quad \text{(A2)}$$

where

$$r^2=(x-z\tan\theta)^2+y^2+z^2$$

is the distance from the point on the track to the element of area on the surface at $\rho\rightarrow(x,y)$. Here, $\beta=1$ if nonreflecting boundary conditions are used, as in Refs. 20 and 26, and $\beta=2$ if reflecting boundary conditions are used as in Refs. 21 and 22.

As is customary, the length variables are scaled by $4\kappa t$, and, in addition, z is scaled by $\cos\theta$ in order to write Eqs. (A1) and (A2) in a simple form. Because of the rapid decay of ε_s at large ρ and t, the yield in Eq. (A1) can be reduced to the form

$$Y=\frac{\bar{\Phi}}{32\pi\kappa}\left[\frac{\beta f_e}{nU}\left[\frac{dE}{dx}\right]_e\right]^2 I , \quad \text{(A3)}$$

where

$$\bar{\Phi}\equiv\int_0^\infty dw\,(1/w^3)\Phi(w) ,$$

with $w=(E_s/nU)$. The changes in the order of integration performed to get this result depend also on Φ going to zero rapidly when ε_s goes to zero.

Note that Eq. (A3) has the quadratic dependence on $(dE/dx)_e$ that is found in the MeV He data. The integral I is

$$I=\frac{8}{\pi^2}\int_{-\infty}^{\infty}dx'\int_{-\infty}^{\infty}dy' f^2(x',y') , \quad \text{(A4)}$$

with

$$f(x',y')=\int_0^\infty dz'\,e^{-I'^2}, \quad r'^2=x'^2+y'^2+z'^2-2x'z'\sin\theta ,$$

with primes indicating the scaled variables. By a series of variable changes, I integrates analytically,

$$I=\frac{4}{\pi}\frac{1}{\cos\theta}\tan^{-1}\left[\frac{1}{\cos\theta}\right] , \quad \text{(A5a)}$$

which at small $(\cos\theta^{-1}-1)$ (Ref. 14) is approximately

$$I\approx\frac{1}{(\cos\theta)^n} , \quad \text{(A5b)}$$

with

$$n=1+2/\pi=1.637$$

very close to the measured values. Claussen[21] estimated $n=1.5$ for a particular variation of the diffusivity on the local energy density.

In this formulation no mechanism has been specified other than that the sum of the net "energy" at the surface from a narrow track of excitation produces the yield by a process contained in the integral $\bar{\Phi}$. Further, no additional time dependence is assumed to occur in the activated process or the transport process. The principle constraints are that the integral $\bar{\Phi}$ exists and the conditions for changing the order of integration are satisfied. These imply that $\Phi(w)$ decays much faster than w^2 when w goes to zero and that $\Phi(w)$ increases slower than w^2 at large w. In this formulation it is also not necessary that "heat" diffuses, rather the excited state energy can diffuse to the surface and operate via $\bar{\Phi}$. In fact, the form for the integral I, Eq. (A4), is such that an effect which decays as e^{-r^2} from each source can act quadratically to produce the angular dependence obtained in Eq. (A5a) without even invoking diffusion. In any case, the measured $n\approx1.64$ is due to the separate excitation events along the particle path acting cooperatively at the surface.

[1]P. Sigmund, in *Sputtering by Particle Bombardment I*, edited by R. Behrisch (Springer, Berlin, 1981), p. 4; Phys. Rev. **184**, 383 (1969).

[2]W. L. Brown, L. J. Lanzerotti, J. M. Poate, and W. M. Augustyniak, Phys. Rev. Lett. **40**, 1027 (1978).

[3]W. L. Brown and R. E. Johnson, Nucl. Instrum. Methods **B13**, 295 (1986).

[4]J. Schou, Nucl. Instrum. Methods **B27**, 188 (1987).

[5]R. E. Johnson and W. L. Brown, Nucl. Instrum. Methods **198**, 103 (1982); **209&210**, 469 (1983).

[6]W. L. Brown, W. M. Augustyniak, E. Simmons, K. J. Marcantonio, L. J. Lanzerotti, R. E. Johnson, J. W. Boring, C. T. Riemann, G. Foti, and V. Pironello, Nucl. Instrum. Methods **198**, 1 (1982).

[7]W. L. Brown, W. M. Augustyniak, K. J. Marcantonio, E. H. Simmons, J. W. Boring, R. E. Johnson, and C. T. Reimann, Nucl. Instrum. Methods **B1**, 307 (1984).

[8]L. J. Lanzerotti, W. L. Brown, W. M. Augustyniak, R. E. Johnson, and T. P. Armstrong, Astrophys. J. **259**, 920 (1982).

[9]W. L. Brown, W. M. Augustyniak, E. Simmons, K. J. Marcantonio, L. J. Lanzerotti, R. E. Johnson, J. W. Boring, C. T. Riemann, G. Foti, and V. Pirronello, Nucl. Instrum. Methods **198**, 1 (1982).

[10]W. L. Brown, L. J. Lanzerotti, K. J. Marcantonio, R. E. Johnson, and C. T. Reimann, Nucl. Instrum. Methods **B14**, 392 (1986).

[11]O. Ellegaard, J. Schou, H. Sørensen, and P. Børgesen, Surf. Sci. **167**, 474 (1986).

[12]F. L. Rook, W. L. Brown, and R. E. Johnson, Surf. Sci. **164**, 625 (1985).

[13]W. L. Brown, G. Foti, L. J. Lanzerotti, J. E. Bower, and R. E. Johnson, Nucl. Instrum. Methods **B19&20**, 899 (1987).

[14]R. E. Johnson, B. Sundqvist, P. Hakansson, A. Hedin, M. Salehpour, and G. Save, Surf. Sci. **179**, 187 (1981).

[15]L. H. Toburen, W. E. Wilson, and R. J. Popowich, Radiat. Res. **82**, 27 (1980).
[16]O. H. Crawford (unpublished).
[17]B. J. Garrison and R. E. Johnson, Surf. Sci. **148**, 388 (1984).
[18]S. K. Allison, Phys. Rev. **109**, 76 (1958).
[19]P. Hakansson, I. Kamensky, and B. Sundqvist, Surf. Sci. **116**, 302 (1982).
[20]R. E. Johnson and R. Evatt, Radiat. Eff. **52**, 181 (1980).
[21]P. Sigmund and C. Claussen, J. Appl. Phys. **52**, 990 (1981).
[22]C. Claussen, Ph.D. thesis, Odense Universtet, 1982.
[23]R. E. Johnson, Int. J. Mass Spectrom. Ion Process. **78**, 357 (1987).
[24]I. S. Bitensky and E. S. Pariles, Nucl. Instrum. Methods **B21**, 26 (1987).
[25]D. B. Chrisey, W. L. Brown, and J. W. Boring (unpublished).
[26]G. Vineyard, Radiat. Eff. **29**, 245 (1976).
[27]C. T. Reimann, W. L. Brown, and R. E. Johnson, Phys. Rev. B **37**, 1455 (1988).